scientific reports

Check for updates

OPEN

Downregulation of Zn-transporters along with Fe and redox imbalance causes growth and photosynthetic disturbance in Zn-deficient tomato

Ahmad Humayan Kabir[1]✉, Mst Salma Akther[1], Milan Skalicky[2]✉, Urmi Das[1], Gholamreza Gohari[3], Marian Brestic[2,4] & Md. Monzur Hossain[1]

Zinc (Zn) deficiency hinders growth and development in tomato. This study unveils the responses of how Zn starvation affects physiological and molecular processes in tomato. Zn deficiency negatively affected the biomass, cellular integrity, and chlorophyll synthesis in tomato. Also, Zn deficiency decreased the maximum yield of PSII, photosynthesis performance index and dissipation energy per active reaction center, although the antenna size, trapping energy efficiency and electron transport flux were stable in Zn-starved leaves. Further, Zn shortage caused a substantial reduction in Zn and Fe concentrations in both roots and shoots along with decreased root Fe-reductase activity accompanied by the downregulation of *Fe-regulated transporter 1*, *Zn transporter-like (LOC100037509)*, and *Zn transporter (LOC101255999)* genes predicted to be localized in the root plasma membrane. The interactome partners of these Zn transporters are predominantly associated with root-specific metal transporter, ferric-chelate reductase, *BHLH* transcriptional regulator, and Zn metal ion transporters, suggesting that Zn homeostasis may be tightly linked to the Fe status along with *BHLH* transcription factor in Zn-deficient tomato. We also noticed elevated $O_2^{\cdot-}$ and H_2O_2 due to Zn deficiency which was consistent with the inefficient antioxidant properties. These findings will be useful in the downstream approach to improve vegetable crops sensitive to Zn-deficiency.

Zinc (Zn) shortage, a scarcity of plant nutrition has an inauspicious consequence on vegetables[1]. With high pH or alkaline stress, there are many lands in different regions across the globe are Zn-deficient[2]. The soil, which contains a sandy texture, as well as less phosphorus, is also deficient in Zn[3]. The plants which are sensitive Zn-starved conditions are often exhibiting reduced growth, dwarf stems, and light chlorosis[4]. The functions of Zn can be found in photosynthetic and gene expression processes besides enzymatic and catalytic activities[5]. Inadequacy of Zn also resulted in a deterioration in plant stomatal activity[1]. In response to the pathogenic invasion of plants, Zn proteins also play a significant role[6]. The insufficiency of Zn in plant-based foods contributes to human malnutrition throughout the world[7].

While generally there is a genotypic difference in Zn-deficiency responses, a plethora of plants are susceptible to Zn deprivation[4,8]. As Zn efficiency mechanisms are somewhat complex in their actions, research has been found a few adaptive features confer Zn deficiency in plants[4,9]. Since it is tough for Zn to penetrate the root cell membranes, therefore the elevation of Zn is attained through transporters at the primary stage[4,8]. The *IRT1*, known as Fe-regulated transporter, is often incited to ameliorate translocation as well as Zn exploitation whenever the plant has possibly Zn or Fe shortcomings[10,11]. *IRT1* is responsible for transporting several minerals such as Zn, Mn, and Fe, even though the pattern of expression varies depending on mineral stresses[12]. Fe and Zn are strictly regulated in plants and they are typically connected owing to the chemical resemblance and *IRT1* non-specificity[13]. Besides, ferric chelate reductase (FCR) activity along with Strategy I responses are induced in Fe-deprived plants, which are generally dicots[14,15]. FCR affects the availability of Fe and could influence the absorption of different types of metals[16]. Hereafter, improvement is declared to conferring the involvement of *ZIP* (Zn transporter) in Fe and Zn uptake[11,17,18], though the evidence in tomato continues to be limited. Pavithra

[1]Department of Botany, University of Rajshahi, Rajshahi 6205, Bangladesh. [2]Department of Botany and Plant Physiology, Faculty of Agrobiology, Food and Natural Resources, Czech University of Life Sciences Prague, Kamycka 129, 165 00 Prague, Czech Republic. [3]Department of Horticultural Sciences, Faculty of Agriculture, University of Maragheh, Maragheh, Iran. [4]Department of Plant Physiology, Slovak University of Agriculture, Nitra, Tr. A. Hlinku 2, 94901 Nitra, Slovakia. ✉email: ahmad.kabir@ru.ac.bd; skalicky@af.czu.cz

et al.[19] classified as low-affinity (*SlZIP5L2*, *SlZIP5L1*, *SlZIP4*, and *SlZIP2*) and high-affinity (*SlZIPL*) Zn transporters in tomato. Nevertheless, these explications were tentatively claimed in the shoot instead of root tissue, in which the absorption of metal occurs in plants.

The deficiency of Zn also causes the accumulation of excessive reactive oxygen (ROS) species, which impedes photosynthesis and protein biosynthesis[4,9]. Therefore, elevated detoxifying ROS is one of the pioneer strategies plants often possess in response to abiotic stress. ROS scavenging enzymes play a vital part in controlling reactive radicals to restore the cell's redox balance[9]. Among the enzymes, catalase (CAT) and superoxide dismutase (SOD) were mainly demonstrated to underlie ROS scavenging in Zn-deprived plants[20]. Besides, ascorbate peroxidase (APX) is able to transform excessive H_2O_2 into the water in ROS-induced plants[21]. However, the induction of antioxidant resistance largely depends on the plant species/genotypes.

Tomato (*Solanum lycopersicum* L.) is known to a high-value crop all over the world[22]. The insufficiency of the inevitable micronutrient Zn adversely affects tomato production worldwide. However, the outcome of low Zn availability on the physiological and molecular repercussions for which tomato plants suffer from growth retardation remains entirely unfamiliar. In this manner, this study aims at unveiling the reasons for dysfunctions found in the tomato plant under Zn deficiency supported by the different biochemical and molecular investigations.

Materials and methods

Plant cultivation technique. As obvious from a previous study[23], Zn-sensitive tomato cultivar (cv. Ratan) was used for this study. The periphery of the seeds was cleaned up with 70% ethyl alcohol for 3 min, followed by doubled Milli-Q water before transferred to the germination tray at room temperature. The sprouted three-days homogeneous plantlets thereafter were transferred to the hydroponic solution at pH 6.0[24], as it is formerly narrated (μM): KNO_3 (1600), $Ca(NO_3)_2.4H_2O$ (600), KH_2PO_4 (100), $MgSO_4.7H_2O$ (200), KCl (50), H_3BO_3 (25), Fe-EDTA (20), $MnSO_4.4H_2O$ (2), $Na_2MoO_4.2H_2O$ (0.5) and $CuSO_4.5H_2O$ (0.5). Furthermore, $ZnSO_4$ has been used as follows[8]: 2.0 μM (Zn-sufficient or control) and 0.01 μM (Zn-deficient). The pH of the solution was adjusted to 6.0 using KOH/HCl and the solution was changed in every 4 days interval. The seedlings were grown in an aerated plastic container (1.2 L) for each treatment having 9 plants/container in an indoor growth chamber. Each seedling was inserted through foam attached to a cut centrifuge tube, exposing the roots to the solution. The growth chamber was strictly controlled with photoperiod 14 h dark/10 h light at ± 26 °C, 65% air humidity, and 200 μmol m^{-2} s^{-1} light intensity. The plants were cultivated for 14d before harvesting for data analysis.

Characterization of morphology, photosynthesis and Fe chelate reductase activity. A digital caliper was used for measuring the length of the root and shoot. The dry weight of root and shoot was recorded after drying for 3 days at 80 °C in an electric oven. For measuring the chlorophyll score of young leaves, a SPAD meter was used (Minolta, Japan). Furthermore, photosynthesis biophysics through chlorophyll fluorescence kinetic (OJIP), such as maximum quantum yield of PSII (FvFm), photosynthesis performance index (Pi_ABS), dissipation energy per active reaction center (DIo/RC), absorption flux/effective antenna size of an active reaction center (ABS/RC), electron transporter flux further than QA DIo/RC (ET2o/RC) and trapped energy flux leading to a reduction of QA (TRo/RC) was recorded on young leaves kept for 1 h at dark using FluorPen FP 100 (Photon Systems Instruments, Czech Republic).

Fe chelate reductase activity (FCR) activity in roots was determined in roots by ferrozine assay[15]. Briefly, the 0.2 mM $CaSO_4$ followed by Milli-Q water washed off the root surface. The roots samples were then homogenized with 1 ml of assay mixture (100 mM Fe(III) EDTA, 0.10 mmol MES-NaOH (pH 5.5), 300 mM ferrozine). The samples and blank tubes (without assay mixture) were incubated in the dark for 20 min at 25 °C. Finally, aliquots were read at 562 nm. The FCR activity was determined by using the molar extinction coefficient (27.9 mM^{-1} cm^{-1}) of ferrozine.

Elemental analysis in root and shoot. Tomato roots were rinsed out once with 0.1 mM $CaSO_4$ and several instances with Milli-Q water to eliminate external components. The roots and shoots were then desiccated individually at 70 °C in an oven for 3d. The samples were then digested with $HNO_3/HClO_4$, 3:1 v/v. Afterward, the Zn and Fe were tested by means of atomic absorption spectroscopy (AA-6800, SHIMADZU).

Determination of soluble protein. In brief, fresh root and shoot were ground with tris–HCl buffer (50 mM, pH 7.5), 2 mM EDTA and 0.04% (v/v) β-mercaptoethanol. In order to separate the transparent fluid portion, the crude specimens were centrifuged for 10 min at 12,000 rpm (MicroCL 21, Thermo Scientific, United States). Subsequently, 1 ml of Coomassie Brilliant Blue (CBB) was diluted to 100 μl protein extract before measuring the absorbance at 595 nm. A bovine serum albumin (BSA) curve was modeled for estimating the total soluble protein as described by Bradford assay[25].

Assessment of electrolyte leakage and cell death. The ultimate consequence of damage of the cell membrane integrity in both root and shoot were measured by using a conductivity meter with some modifications[26]. Root and shoot surface components were washed with deionized water. Thereafter, the freshly harvested samples were transferred into a beaker filled with 20 ml deionized water and kept at 25 °C for 2 h. Later, the solution's electrical conductivity (EC1) was calculated. Afterward, the samples were heated in a water bath for 20 min at 95 °C then soothed at 25 °C before recording the final electrical conductivity (EC2). The electrolyte leakage was then determined as follows: = (EC1/EC2) × 100 (%).

Evans blue was determined to account for the cell death rate with some modifications[27]. The entire fresh root and shoot were placed into 2 mL of Evan's blue mixture for 15 min. The samples were then mixed with 80% ethyl alcohol and placed at room temperature for 10 min. Afterward, the solutions were incubated in a water bath for

15 min at 50 °C and were further centrifuged for 10 min at 12,000 rpm (MicroCL 21, Thermo Scientific, United States). The supernatant was then transferred into a new centrifuge tube before measuring the absorbance at 600 nm. Eventually, the % of cell death was calculated.

Analysis of O_2^-, H_2O_2 and lipid peroxidase. The superoxide (O_2^-) was tested as mentioned previously[28]. Briefly, the fresh samples (0.1 g) were washed with water, homogenized with chilled K-phosphate buffer (10 mM), and centrifuged at 12,000 rpm at 4 °C for 10 min. The clear supernatant (100 µl) was mixed up with 1 ml of assay solution with 0.5 mM XTT sodium salt and 50 mM Tris–HCl (pH 7.5). Finally, the solution's absorbance was read at 580 nm and the superoxide (O_2^-) was calculated by the coefficient of extinction $2.16 \times 104\ M^{-1}\ cm^{-1}$). The H_2O_2 accumulation was measured, utilizing 0.1% $C_2HCl_3O_2$[29]. The fresh samples (0.1 g) were ground with a mortar and pestle in 0.1% $C_2HCl_3O_2$ and further centrifuged at 10,000 rpm for 15 min. The top aqueous segment (100 µl) was appended with assay solution supplemented with 10 mM K-phosphate (pH 7.0), 1 M KI. The samples were then adapted to dark for 1 h before recording the absorbance at 390 nm (Shimadzu UV-1650PC). For the determination of lipid peroxidase activity, the fresh samples (0.1 g) were homogenized in 20% $C_2HCl_3O_2$ incorporated with 0.5% $C_4H_4N_2O_2S$ mixture. The clear supernatant (1 ml) was warmed at 95 °C for 30 min in a water bath and subsequently chilled on ice. The samples were then centrifuged at 12,000 rpm for 10 min. The optical density of the samples was monitored 532 and 600 nm (60S UV–Visible Spectrophotometer, Thermo Scientific, United States). The lipid peroxidase activity was determined according to the coefficient of molar extinction 155 mmol L^{-1} cm[30].

Gene expression and bioinformatics analysis. The total RNA was isolated from the fresh roots as described by SV total RNA isolation system (Promega, USA). The quantified RNA was then converted to cDNA using the cDNA synthesis kit (Promega, USA) before performing real-time PCR analysis in an ECO real-time PCR system (Illumina, USA) using gene-specific primers for iron-regulated transporter 1, zinc transporter-like (*LOC100037509*) and zinc transporter (*LOC101255999*) (Table S1). The PCR reactions were set as follows: 95 °C for 3 min, followed by 40 cycles at 95 °C for 10 s, 57 °C for 30 s. The relative expression of candidate genes was calculated by the dd – ΔCt method considered *Actin* as an internal control. Further, the sub-cellular localization of these genes was predicted by CELLO v.2.5. The interactome networks of iron-regulated transporter 1, zinc transporter-like (*LOC100037509*) and zinc transporter (*LOC101255999*) were generated based on the physical interactions among molecules (protein–protein interactions) using the STRING server (http://string-db.org) visualized in Cytoscape[31].

Activities of antioxidant enzymes. In brief, the root and shoot samples (0.1 g) were independently homogenized with 100 mM phosphate (pH 7.0) in a mortar and pestle. The homogenate was centrifuged at 8000 rpm for 10 min (MicroCL 21, Thermo Scientific, United States)., and the transparent portion was collected for analysis. We first analyzed the SOD activity by mixing the plant extract (100 µl) with 0.1 mM of EDTA, 50 mM of $NaHCO_3$ (pH 9.8), and 0.6 mM of epinephrine[32]. After 4 min, the adrenochrome confirmation was read at 475 in a spectrophotometer. Secondly, the plant extract (100 µl) was supplemented with 1 ml of assay solution with 0.1 mM EDTA, 0.1 mM H_2O_2, 0.5 mM ascorbic acid, and 50 mM phosphate[33]. The absorbance of the mixture was then observed at 290 nm and thereafter calculated for APX activity by extinction coefficient ($2.8\ mM^{-1}\ cm^{-1}$). Besides, 100 µl extract was mixed up with 100 mM phosphate buffer and 6% hydrogen peroxide solution. The absorbance was read twice in 30 s interval and thereafter calculated for the activity of CAT using a coefficient of $0.036\ mM^{-1}\ cm^{-1}$). Lastly, 100 mM phosphate, 1 mM EDTA, 20 mM GSSG and 0.2 mM NADPH added individually to 100 µL of plant extract. The reaction was initiated by GSSG, and absorption was reduced by NADPH-oxidation at 340 nm. The calculation of GR activity was then performed by the extinction coefficient ($6.12\ mM^{-1}\ cm^{-1}$)[34].

Statistical analysis. We opted for a completely randomized block design (CRBD) in plant cultivation. Three independent biological replications were considered for data analysis. Each experiment was performed at least three times to check whether the results were reproducible. The statistical significance of mean was evaluated by Microsoft Excel 2010 at $p \leq 0.05$ by *t*-test. Figures were plotted by using GraphPad Prism (V. 6.0) software.

Results

Changes in morphology, photosynthetic parameters and FCR activity. Zn deficiency showed a significant reduction in the root (root length, dry root weight) and in the shoot characteristics (shoot height, dry shoot weight) in Ratan than untreated controls (Fig. 1a–e). In addition, Zn-deprivation led to a significant reduction in the SPAD score as opposed to control plants (Fig. 3a). Besides, the leaf chlorophyll score and root FCR activity significantly decreased owing to Zn-deprivation relative to controls (Fig. 1f,g). The Fv/Fm and Pi_ABS values showed a large decrease in young leaves as a result of Zn-shortage as opposed to controls (Fig. 2a,b). However, the DIo/RC value considerably increased in Zn-starved leaves in contrast to controls (Fig. 2c). OJIP analysis showed no changes in ABS/RC, ET2o/RC, and TRo/RC values between Zn + and Zn− conditions (Fig. 2d–f).

Changes in stress indicators. In Ratan, the total soluble protein in the root and shoot remained unchanged due to Zn-deprivation in contrast to plants grown with optimal Zn (Fig. 3a). Furthermore, cell death (%) and electrolyte leakage in either root or shoot increased significantly following Zn shortage relative to controls in Ratan (Fig. 3b,c). Although the O_2^- showed no changes in the root, the accumulation of this ROS significantly increased following Zn starvation relative to Zn-sufficient plants (Fig. 3d). The H_2O_2 in root and shoot of tomato

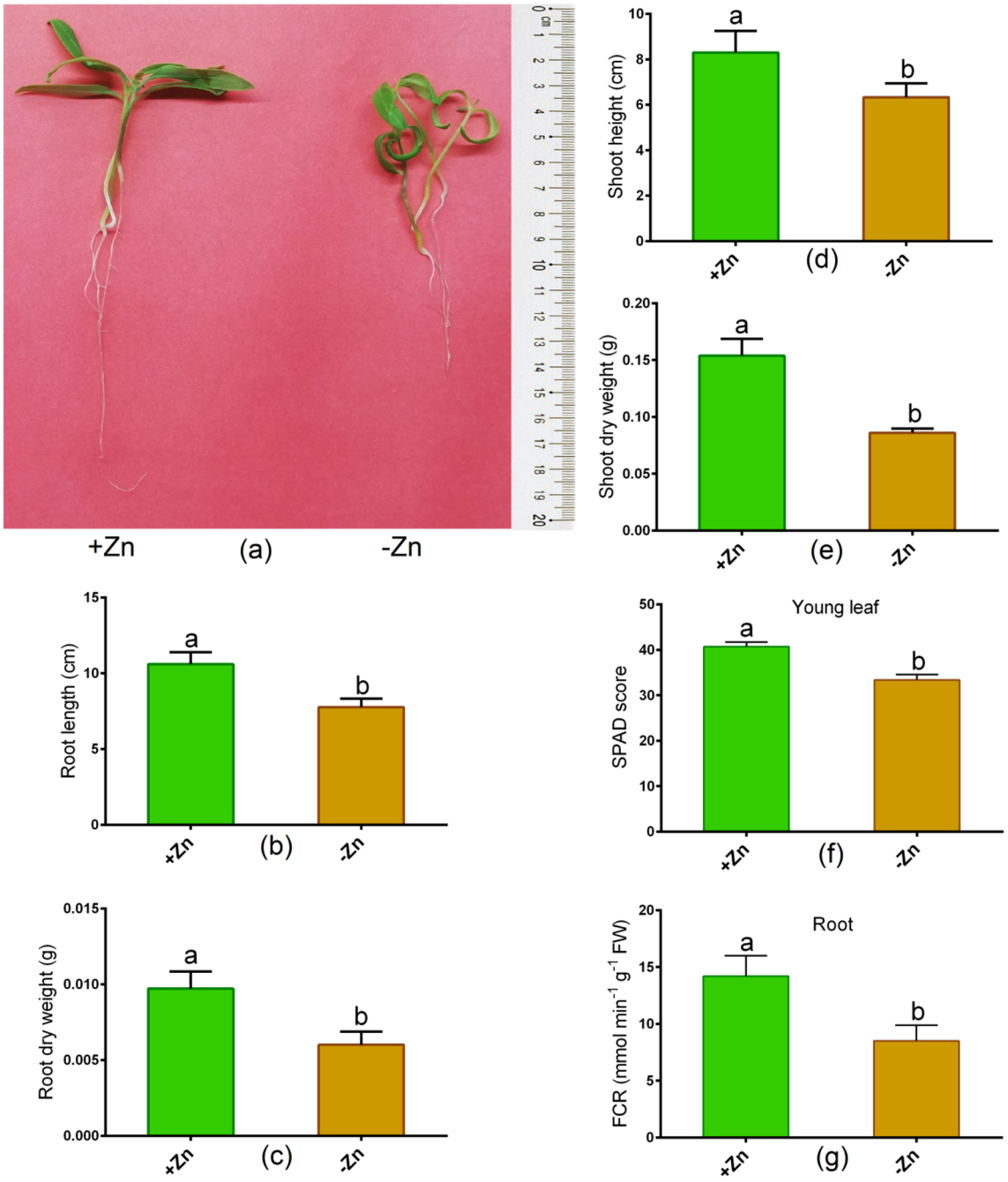

Figure 1. Phenotype (**a**), root length (**b**), root dry weight (**c**), shoot height (**d**), shoot dry weight (**e**), leaf chlorophyll score (**f**) and root FCR (ferric chelate reductase) activity (**g**) in tomato cultivated under Zn-sufficient and Zn-deficient conditions for 14 days. Different letters indicate significant differences between means ± SD of treatments ($p < 0.05$, n = 3).

significantly increased owing to Zn-deficiency relative to controls (Fig. 3e). However, the lipid peroxidase activity remained unchanged between Zn-sufficient and Zn-deficiency conditions (Fig. 3f).

Metal analysis, gene expression pattern and in silico validation. The concentrations of Fe and Zn showed a significant decrease in root and shoot because of Zn insufficiency relative to Zn-sufficient plants (Table 1). To validate the metal analysis, we analyzed the expression pattern of key Zn transporters in tomato roots. In real-time PCR analysis, Fe-regulated transporter 1 showed a substantial downregulation in roots subjected to Zn-shortage as opposed to Zn-sufficient plants (Fig. 4a). Additionally, the expressions of Zn transporter-like (*LOC100037509*) and Zn transporter (*LOC101255999*) genes were significantly downregulated due to Zn shortage in roots compared with Zn sufficient controls (Fig. 4a).

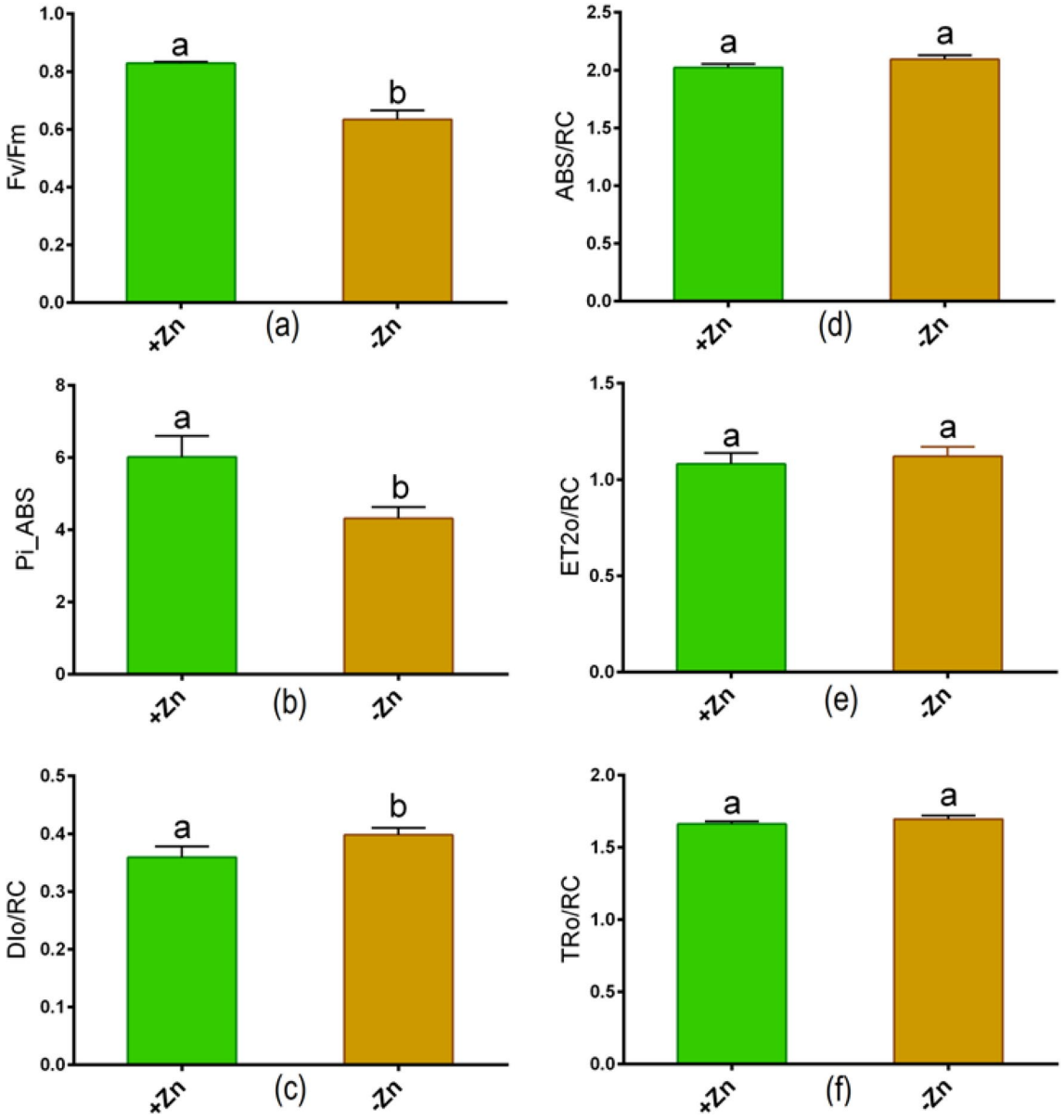

Figure 2. Chlorophyll fluorescence parameters: (**a**) maximum quantum yield of PSII (Fv/Fm), (**b**) photosynthesis performance index (Pi_ABS), (**c**) dissipation energy per active reaction center (DIo/RC), (**d**) absorption flux/effective antenna size of an active reaction center (ABS/RC), (**e**) electron transport flux further than QA DIo/RC (ET2o/RC) and (**f**) trapped energy flux leading to a reduction of QA (TRo/RC) in young leaves of tomato cultivated Zn-sufficient and Zn-deficient conditions for 14 days. Different letters indicate significant differences between means ± SD of treatments ($p < 0.05$, n = 3).

CELLO predictor showed that these genes are localized in the plasma membrane of the root resulting highest reliability score (Fig. 4b). STRING showed five putative interaction partners of iron-regulated transporter 1, which include *NRAMP1* (root-specific metal transporter), *NRAMP3* (metal transporter), *FRO1* (ferric-chelate reductase), *fer* (BHLH transcriptional regulator) and *CHLN* (nicotianamine synthase) genes (Fig. 5). In addition, zinc transporter-like (LOC100037509) are closely linked in a partnership with *Solyc05g008340.2.1* (ZIP metal ion transporter family), *101,253,965* (ZIP metal ion transporter family), *101,253,075* (ATPase EI), *101,255,936* (WCRKC thioredoxin) and *101,262,011* (Zn-binding dehydrogenase family protein). Interactome analysis also showed close interactions of Zn transporter (LOC101255999) with *Solyc05g008340.2.1* (ZIP metal ion transporter family), *101,253,965* (ZIP metal ion transporter family), *Solyc01g087530.2.1* (ZIP metal ion transporter family), *fer* (BHLH transcriptional regulator) and *101,245,241* (major facilitator superfamily protein) genes (Fig. 5).

Changes in antioxidant enzymes. We have analyzed the different antioxidant enzymes, whether this tomato cultivar does have antioxidant properties to withstand oxidative damage. Results showed that CAT, SOD, APX, and GR activities remained unchanged in roots, but these enzymes significantly reduced due to Zn-starvation in comparison with Zn-sufficient plants (Fig. 6a–d).

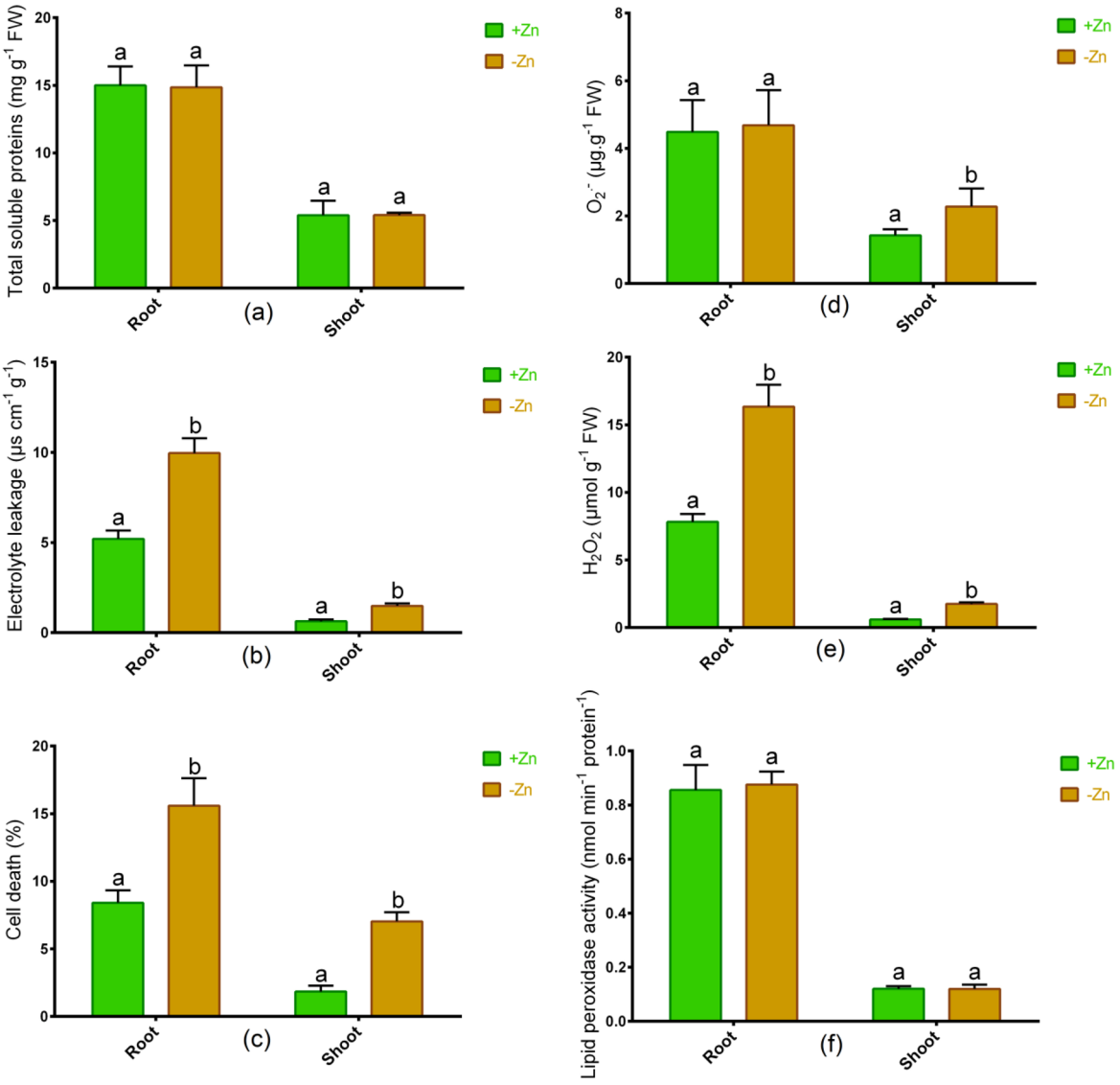

Figure 3. Total soluble proteins (**a**), electrolyte leakage (**b**), cell death % (**c**), O_2^- (**d**), H_2O_2 (**e**) and lipid peroxidase activity (**f**) in roots and shoots of tomato cultivated under Zn-sufficient and Zn-deficient conditions for 14 days. Different letters indicate significant differences between means ± SD of treatments ($p < 0.05$, n = 3).

Parameters	Root		Shoot	
	+Zn	−Zn	+Zn	−Zn
Zn	217.7 ± 17.8a	135.17 ± 14.1b	127.2 ± 17.1a	69.9 ± 12.8b
Fe	254.1 ± 21.3a	117 ± 16.1b	101.6 ± 12.2a	38.6 ± 9.7b

Table 1. Zn and Fe concentrations (mg kg^{-1}) in roots and shoots of tomato cultivated under Zn-sufficient and Zn-deficient hydroponic conditions for 14 days. Different letters indicate significant differences between means ± SD of treatments ($p < 0.05$, n = 3).

Discussion

Understanding the mechanistic consequence of mineral deficiency responses is of great importance to initiate crop improvement steps through breeding or genome editing approaches. Long ago[35], gave a tentative sign that tomato Zn uptake is restricted to the root system rather than the aerial part. Since then, extensive studies related to Zn-starved tomato have not been elucidated. This research offers some new insight into improvements in photosynthesis, Zn transporters, and the antioxidant ability for which tomato plants cannot overcome Zn deficiency.

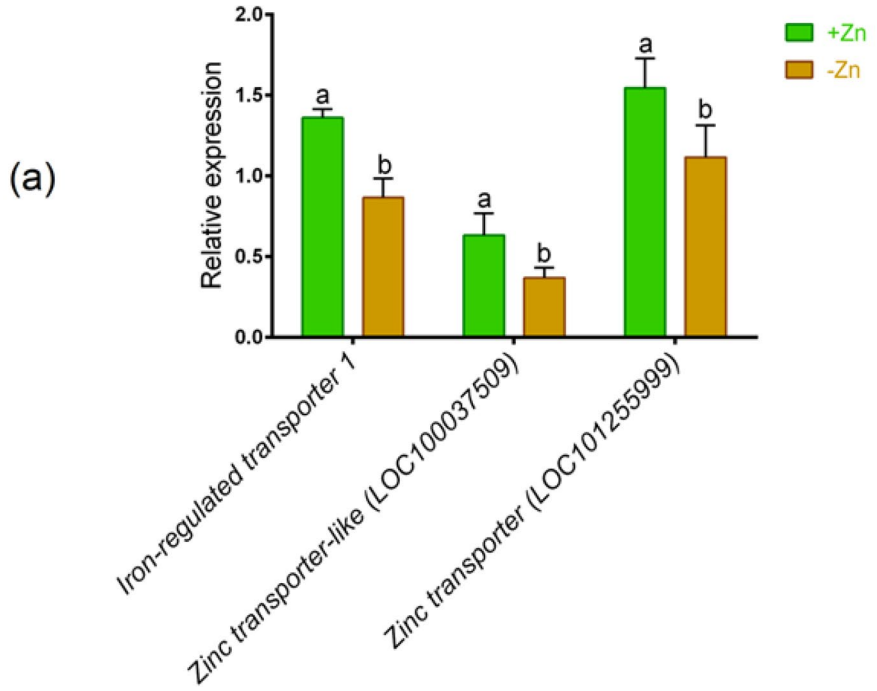

CELLO RESULTS

Iron-regulated transporter 1

LOCALIZATION	RELIABILITY
PlasmaMembrane	0.975
PlasmaMembrane	1.000
PlasmaMembrane	0.908
PlasmaMembrane	0.985
PlasmaMembrane	0.957
PlasmaMembrane	4.825 *
Mitochondrial	0.069
Chloroplast	0.027
Cytoplasmic	0.019
Peroxisomal	0.017
Extracellular	0.014
ER	0.012
Nuclear	0.009
Golgi	0.003
Lysosomal	0.002
Vacuole	0.002
Cytoskeletal	0.001

Zinc-transporter-like (LOC100037509)

LOCALIZATION	RELIABILITY
PlasmaMembrane	0.971
PlasmaMembrane	0.996
PlasmaMembrane	0.938
PlasmaMembrane	0.904
PlasmaMembrane	1.000
PlasmaMembrane	4.809 *
Extracellular	0.115
Lysosomal	0.013
Mitochondrial	0.012
Nuclear	0.012
Cytoplasmic	0.009
Chloroplast	0.007
Peroxisomal	0.007
ER	0.006
Golgi	0.005
Vacuole	0.004
Cytoskeletal	0.001

Zinc transporter (LOC101255999)

LOCALIZATION	RELIABILITY
PlasmaMembrane	0.997
PlasmaMembrane	1.000
PlasmaMembrane	0.998
PlasmaMembrane	0.767
PlasmaMembrane	0.999
PlasmaMembrane	4.761 *
Extracellular	0.187
Lysosomal	0.017
Nuclear	0.012
ER	0.007
Chloroplast	0.005
Mitochondrial	0.004
Vacuole	0.002
Peroxisomal	0.002
Cytoplasmic	0.002
Golgi	0.001
Cytoskeletal	0.000

(b)

Figure 4. Quantitative expression of iron-regulated transporter 1, zinc transporter-like *(LOC100037509*) and zinc transporter (*LOC101255999*) genes in roots of tomato cultivated under Zn-sufficient and Zn-deficient conditions for 14 days (**a**) and computational sub-cellular localization prediction (**b**). Different letters indicate significant differences between means ± SD of treatments ($p < 0.05$, n = 3).

Morphological and physiological responses. Zn is essential for metabolism and plant growth. Nevertheless, in Zn inefficient Ratan, the absence of adaptive systems to fight Zn deficiency decreased the root and shoot morphological characteristics. This result is consistent with earlier accounts of Zn deficiency in crop plants[8]. In the research of ours, reduced chlorophyll, PSII capability, and photosynthesis performance index were correlated with the morphological features in Ratan. The chlorophyll value decreases along with Fv/Fm and Pi ABS, indicating that Ratan plants were unable to regulate PSII mechanisms under Zn deficiency. Furthermore, the increase of DIo/RC suggests that Zn-deficiency results in ineffective energy management, which is correlated with the reduced photosynthetic efficiency in leaves of Zn-deprived tomato. Zn functions during photosynthesis when CO_2 is fixed, although chloroplast and photosynthesis can be impaired under deficiency[36,37]. Several cellular dysfunctions and damages related to plant abiotic stress. In this particular research, while low Zn did not affect overall soluble protein-rich, Ratan displayed a tremendous rise in cell death as well as membrane damage and accumulation of H_2O_2 in reaction to Zn deficiency. Membrane leakage and cell death are typical effects of abiotic stress[8,38]. Therefore, our results suggest that an inadequate supply of Zn is one of the features for which Ratan cannot maintain the cellular integrity, morphological, and photosynthesis efficiency subjected to Zn deficiency.

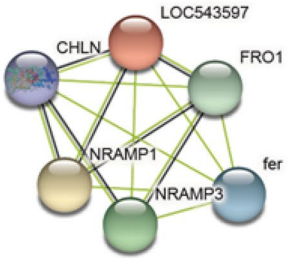

Input:

Iron-regulated transporter 1

Predicted Functional Partners:

		Neighborhood	Gene Fusion	Cooccurence	Coexpression	Experiments	Databases	Textmining	[Homology]	Score
NRAMP1	*Root-specific metal transporter (530 aa)*									0.819
NRAMP3	*Metal transporter (509 aa)*									0.816
FRO1	*Uncharacterized protein; Ferric-chelate reductase (719 aa)*									0.806
fer	*BHLH transcriptional regulator (304 aa)*									0.806
CHLN	*Nicotianamine synthase; Synthesizes nicotianamine, a polyamine that serves as a sensor for the physiological iron status ...*									0.799

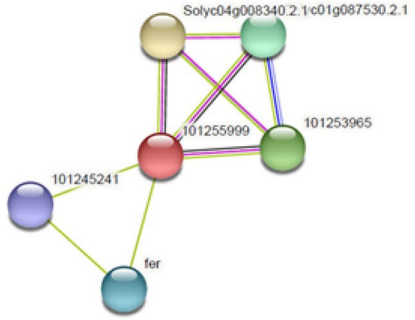

Input:

Zinc transporter-like (LOC100037509)

Predicted Functional Partners:

		Neighborhood	Gene Fusion	Cooccurence	Coexpression	Experiments	Databases	Textmining	[Homology]	Score
Solyc04g008340.2.1	*Uncharacterized protein; ZIP metal ion transporter family (489 aa)*									0.803
101253965	*Uncharacterized protein; ZIP metal ion transporter family (276 aa)*									0.773
Solyc01g087530.2.1	*Uncharacterized protein; ZIP metal ion transporter family (595 aa)*									0.714
fer	*BHLH transcriptional regulator (304 aa)*									0.690
101245241	*Major facilitator superfamily protein (657 aa)*									0.689

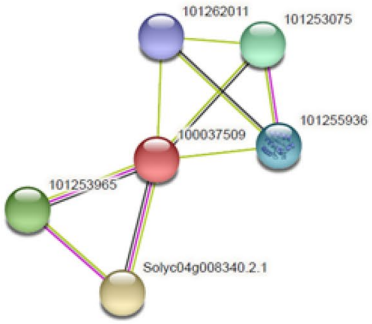

Input:

Zinc transporter (LOC101255999)

Predicted Functional Partners:

		Neighborhood	Gene Fusion	Cooccurence	Coexpression	Experiments	Databases	Textmining	[Homology]	Score
Solyc04g008340.2.1	*Uncharacterized protein; ZIP metal ion transporter family (489 aa)*									0.917
101253965	*Uncharacterized protein; ZIP metal ion transporter family (276 aa)*									0.867
101253075	*Uncharacterized protein; ATPase E1 (167 aa)*									0.797
101255936	*Uncharacterized protein; WCRKC thioredoxin 1 (186 aa)*									0.797
101262011	*Zinc-binding dehydrogenase family protein (357 aa)*									0.797

Figure 5. Predicted gene interaction partners of iron-regulated transporter 1, zinc transporter-like (*LOC100037509*) and zinc transporter (*LOC101255999*) genes in tomato. Interactome was generated using Cytoscape for STRING data.

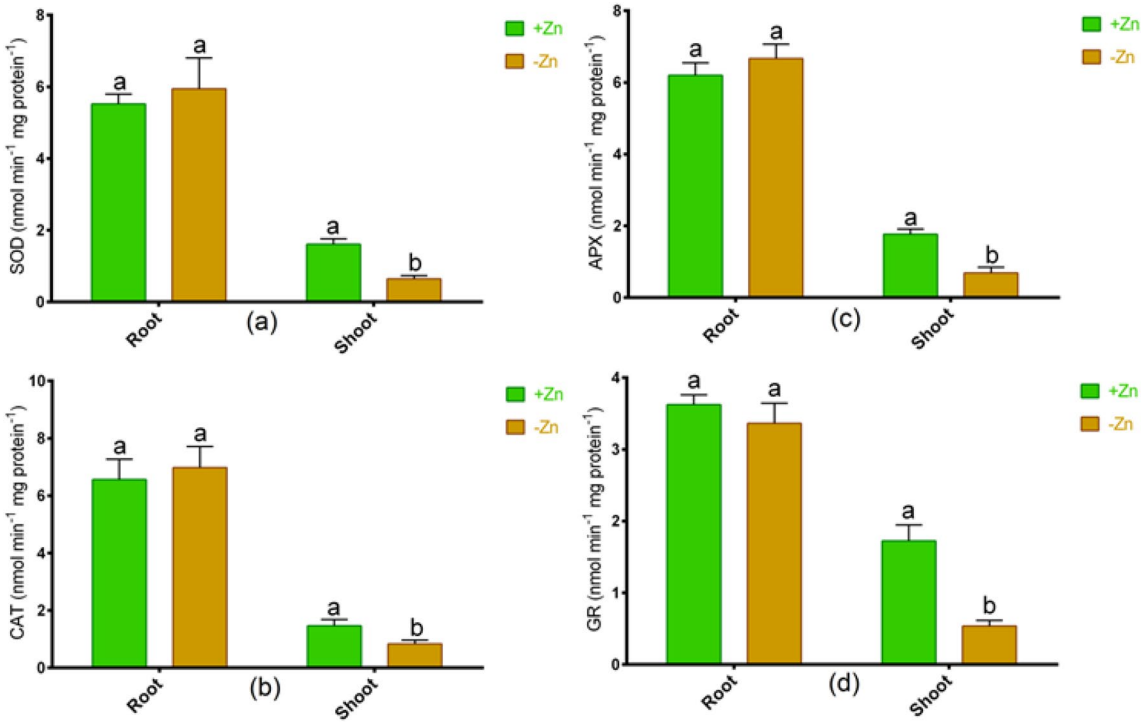

Figure 6. The activities of (**a**) superoxide dismutase (SOD), (**b**) catalase (CAT), (**c**) ascorbate peroxidase (APX) and (**d**) glutathione reductase (GR) in roots and shoots of tomato cultivated under Zn-sufficient and Zn-deficient conditions for 14 days. Different letters indicate significant differences between means ± SD of treatments ($p < 0.05$, n = 3).

Changes of Zn and Fe status. In this study, the concentration of Zn and Fe were simultaneously reduced in response to Zn deficiency in tomato, indicating a complicated Zn and Fe homeostasis response. The rapid decrease of root and shot Zn and Fe concentration in Ratan shows that Zn homeostasis cannot be held under Zn hunger by this genotype. Differential tissue Zn levels have been displayed in a few species of plants that are different in response to Zn scarcity[39]. In the cytosol, *IRT* and *ZIP* proteins are mostly associated with Zn delivery[40,41]. Previous studies demonstrate that Zn deficiency also caused Fe deficiency as plants prevent the transfer of Fe from root to shoot[42,43]. Pavithra et al.[19] emphasized the involvement of shoot showing differential expression of Zn transporters. However, it is slightly confusing as most of the Zn-acquisition genes are localized in the plasma membrane of roots as predicted by the localization predictor. We have therefore carried out a focused analysis on the pattern of expression of *IRT* and *ZIP* in tomato roots. Fe-regulated carrier, Fe-regulated transporter 1, has shown major downregulation in the roots of Ratan, inducing its susceptibility to Zn deficiency. Originally, *IRT1* was identified as a Fe transporter, but complementation and uptake studies revealed its involvement in Mn and Zn in addition to Fe[10,44]. In this study, both Zn transporter-like (*LOC100037509*) and Zn transporter (*LOC101255999*) genes showed a substantial decrease in Ratan root expression patterns that could help to render the Zn root system inefficient for Zn regulation. On the contrary, the induction of ZIP transporter occurs in root or leaf, depending on the plant species/sensitivity[45]. These genes can be good candidates for further functional characterization of Zn-transporter in tomato through genome editing and yeast complementation assay.

The localization of Zn transporters was further validated by the computational prediction. The CELLO analysis predicts that all of these tomato Zn transporters are localized in the plasma membrane which is in agreement with wet-lab experiments reported previously in various plants[46,47]. Ion and solute fluxes underpin inorganic mineral nutrient uptake at the plasma membrane, thereby triggering changes in second messengers such as cytosolic-free Ca^{2+} concentrations in cell[48]. The interactome map further suggests that the Zn transporters in tomato are associated with some genes related to metal ion transporter and transcription factor. The Fe-regulated transporter 1 in tomato is in close partnership with metal transporter (*NRAMP1*, *NRAMP2*), Fe reductase gene (*FRO1*), *fer* transcription factor, and nicotianamine synthase (*CHLN*) genes. Previous studies also demonstrated that the *BHLH068* transcription factor via interaction with *FER* along with *IRT1, NRAMP1* and *FRO1* is involved in iron homeostasis in tomato[49]. Further, *CHLN* encodes nicotianamine forming a complex with Fe^{2+} for the distribution of Fe in plants[50]. The defect in *FER* mutant caused dramatic downregulation of Fe-uptake genes (*IRT1*, *FRO1*) in tomato; however, the molecular mechanism remains unclear[46]. However, *FER*-like transcription factor FIT, expressed in roots was associated with *FRO2* and *IRT1* genes in Arabidopsis[51]. In order to bind to the promoters of *IRT1* and *FRO2*, this *FIT* is not able to act alone but must form a heterodimer with other bHLH proteins, as shown in yeast[52,53]. It is, therefore, possible that Zn-deficiency is associated with the coordination of Fe homeostasis in tomato. Consistently, this study also suggests the involvement of *ZIP* metal ion transporter and *BHLH* transcription factor with Zn transporters in tomato. Overall, this interactome analysis might provide

essential background for functional genomics studies in characterizing transporters and transcription factors underlying Zn-deficiency responses in tomatoes.

Oxidative damage and antioxidant response. In this study, the $O_2^{\cdot-}$ was higher in the roots than in the shoot but significantly decreased in the shoot due to Zn-deficiency, which may be linked to elevated SOD activity. Further, H_2O_2 is a key ROS indication substantially induced in tomato following Zn starvation. The increases in ion flux and gene expression are part of H_2O_2 in plants[43,54]. The degradation of elevated H_2O_2 into less reactive molecules is frequently correlated with CAT[55]. Hacisalihoglu et al.[56] reported that Zn-efficiency is allied with the Zn-SOD enzyme in wheat. In this study, Ratan showed a consistent decline in antioxidant enzymes that are known to inhibit H_2O_2 in the shoot in response to Zn deficiency. Further, APX and GR also showed no induction in tomato subjected to Zn-starvation, suggesting that inefficiency to ROS mitigation is possibly related to the damage of chloroplasts and cellular proteins. Cells are also prone to ROS pools due to abiotic stresses, not just chloroplasts involved in energy production[57]. It implies that ROS scavenging is not present actively in this Zn-deficiency sensitive tomato, especially in the shoot, to combat Zn deficiency. Thus, it pinpoints that the increase of ROS and the decrease in chlorophyll synthesis in Ratan is correlated with the photosynthesis inefficiency in leaves. However, the ROS regulation in plant cells may vary on the species and cultivar of species under Zn deficiency.

Conclusion

Zn deficiency showed a substantial reduction in plant biomass, photosynthetic efficiency, and cellular damage in Zn-deficiency sensitive cultivar (Ratan). The expression of iron-regulated transporter 1, zinc transporter-like (*LOC100037509*) and zinc transporter (*LOC101255999*) significantly decreased following Zn-deprivation resulted in a substantial decrease in Zn and Fe status in either root or shoot of tomato. Although the metal uptake in plants depends on many genes and the activity of the encoded protein, these two Zn-transporters may encourage further research regulating Zn-efficiency in tomato. Furthermore, the morpho-physiological retardation was consistent with the inefficiency of antioxidant defense to cope with the elevated oxidative injuries. This outcome will help to clarify our understanding of Zn deficiency more effectively to accelerate breeding or genome-editing program to improve Zn-deficiency tolerance in tomato for human nutrition.

Data availability

All data of the manuscript are available.

Received: 1 December 2020; Accepted: 4 March 2021
Published online: 16 March 2021

References

1. Mattiello, E. M., Ruiz, H. A., Neves, J. C. L., Ventrella, M. C. & Araújo, W. L. Zinc deficiency affects physiological and anatomical characteristics in maize leaves. *J. Plant Physiol.* https://doi.org/10.1016/j.jplph.2015.05.014 (2015).
2. Scharwies, J. D. & Dinneny, J. R. Water transport, perception, and response in plants. *J. Plant Res.* https://doi.org/10.1007/s10265-019-01089-8 (2019).
3. Bandyopadhyay, T., Mehra, P., Hairat, S. & Giri, J. Morpho-physiological and transcriptome profiling reveal novel zinc deficiency-responsive genes in rice. *Funct. Integr. Genomics* **17**, 565–581 (2017).
4. Khatun, M. A. *et al.* Zinc deficiency tolerance in maize is associated with the up-regulation of Zn transporter genes and antioxidant activities. *Plant Biol.* https://doi.org/10.1111/plb.12837 (2018).
5. Tang, L. *et al.* Transcriptional up-regulation of genes involved in photosynthesis of the Zn/Cd hyperaccumulator Sedum alfredii in response to zinc and cadmium. *Chemosphere* https://doi.org/10.1016/j.chemosphere.2016.08.026 (2016).
6. Cabot, C. *et al.* A role for zinc in plant defense against pathogens and herbivores. *Front. Plant Sci.* **10**, 2 (2019).
7. Millward, D. J. Nutrition, infection and stunting: The roles of deficiencies of individual nutrients and foods, and of inflammation, as determinants of reduced linear growth of children. *Nutr. Res. Rev.* **30**, 50–72 (2017).
8. Kabir, A. H., Hossain, M. M., Khatun, M. A., Sarkar, M. R. & Haider, S. A. Biochemical and molecular mechanisms associated with zn deficiency tolerance and signaling in rice (*Oryza sativa* L.). *J. Plant Interact.* https://doi.org/10.1080/17429145.2017.1392626 (2017).
9. Höller, S., Meyer, A. & Frei, M. Zinc deficiency differentially affects redox homeostasis of rice genotypes contrasting in ascorbate level. *J. Plant Physiol.* https://doi.org/10.1016/j.jplph.2014.08.012 (2014).
10. Lin, Y.-F. *et al.* Arabidopsis IRT3 is a zinc-regulated and plasma membrane localized zinc/iron transporter. *New Phytol.* **182**, 392–404 (2009).
11. Ma, X. *et al.* Genome-wide analysis of zinc- and iron-regulated transporter-like protein family members in apple and functional validation of ZIP10. *Biometals* https://doi.org/10.1007/s10534-019-00203-6 (2019).
12. Durmaz, E. *et al.* Expression and cellular localization of ZIP1 transporter under zinc deficiency in wild emmer wheat. *Plant Mol. Biol. Rep.* https://doi.org/10.1007/s11105-010-0264-3 (2011).
13. Sinclair, S. A. & Krämer, U. The zinc homeostasis network of land plants. *Biochim. Biophys. Acta Mol. Cell Res.* https://doi.org/10.1016/j.bbamcr.2012.05.016 (2012).
14. Kabir, A. H., Paltridge, N. G., Able, A. J., Paull, J. G. & Stangoulis, J. C. R. Natural variation for Fe-efficiency is associated with upregulation of Strategy I mechanisms and enhanced citrate and ethylene synthesis in *Pisum sativum* L. *Planta* https://doi.org/10.1007/s00425-011-1583-9 (2012).
15. Kabir, A. H., Rahman, M. M., Haider, S. A. & Paul, N. K. Mechanisms associated with differential tolerance to Fe deficiency in okra (Abelmoschus esculentus Moench). *Environ. Exp. Bot.* https://doi.org/10.1016/j.envexpbot.2014.11.011 (2015).
16. Morrissey, J. & Guerinot, M. L. Iron uptake and transport in plants: The good, the bad, and the ionome. *Chem. Rev.* **109**, 4553–4567 (2009).
17. Li, S. *et al.* Constitutive expression of the ZmZIP7 in Arabidopsis alters metal homeostasis and increases Fe and Zn content. *Plant Physiol. Biochem.* https://doi.org/10.1016/j.plaphy.2016.04.044 (2016).
18. Bastow, E. L. *et al.* Vacuolar iron stores gated by NRAMP3 and NRAMP4 are the primary source of iron in germinating seeds. *Plant Physiol.* **177**, 1267–1276 (2018).

19. Pavithra, G. J. *et al.* Comparative growth responses and transcript profiling of zinc transporters in two tomato varieties under different zinc treatments. *Indian J. Plant Physiol.* https://doi.org/10.1007/s40502-016-0210-y (2016).
20. Arenas-Lago, D., Carvalho, L. C., Santos, E. S. & Abreu, M. M. The physiological mechanisms underlying the ability of *Cistus monspeliensis* L. from São Domingos mine to withstand high Zn concentrations in soils. *Ecotoxicol. Environ. Saf.* https://doi.org/10.1016/j.ecoenv.2016.03.041 (2016).
21. Zhang, L. *et al.* Overexpression of the glutathione peroxidase 5 (RcGPX5) gene from rhodiola crenulata increases drought tolerance in salvia miltiorrhiza. *Front. Plant Sci.* **9**, 2 (2019).
22. Khadka, R. B., Marasini, M., Rawal, R., Gautam, D. M. & Acedo, A. L. Effects of variety and postharvest handling practices on microbial population at different stages of the value chain of fresh tomato (*Solanum lycopersicum*) in Western Terai of Nepal. *Biomed Res. Int.* https://doi.org/10.1155/2017/7148076 (2017).
23. Akther, M. S. *et al.* Regulation of Zn uptake and redox status confers Zn deficiency tolerance in tomato. *Sci. Hortic. (Amsterdam).* https://doi.org/10.1016/j.scienta.2020.109624 (2020).
24. Hoagland, D. R. & Arnon, D. I. *The water-culture method for growing plants without soil. Circular. California Agricultural Experiment Station 347. Circular 347. California Agricultural Experiment Station* (1950).
25. Guy, C., Haskell, D., Neven, L., Klein, P. & Smelser, C. Hydration-state-responsive proteins link cold and drought stress in spinach. *Planta* **188**, 265–270 (1992).
26. Lutts, S., Kinet, J. M. & Bouharmont, J. NaCl-induced senescence in leaves of rice (*Oryza sativa* L.) cultivars differing in salinity resistance. *Ann. Bot.* https://doi.org/10.1006/anbo.1996.0134 (1996).
27. Zhao, J., Fujita, K. & Sakai, K. Oxidative stress in plant cell culture: A role in production of β-thujaplicin by *Cupresssus lusitanica* suspension culture. *Biotechnol. Bioeng.* https://doi.org/10.1002/bit.20465 (2005).
28. Hu, L., Li, H., Pang, H. & Fu, J. Responses of antioxidant gene, protein and enzymes to salinity stress in two genotypes of perennial ryegrass (*Lolium perenne*) differing in salt tolerance. *J. Plant Physiol.* https://doi.org/10.1016/j.jplph.2011.08.020 (2012).
29. Alexieva, V., Sergiev, I., Mapelli, S. & Karanov, E. The effect of drought and ultraviolet radiation on growth and stress markers in pea and wheat. *Plant Cell Environ.* https://doi.org/10.1046/j.1365-3040.2001.00778.x (2001).
30. Kosugi, H. & Kikugawa, K. Thiobarbituric acid reaction of aldehydes and oxidized lipids in glacial acetic acid. *Lipids* https://doi.org/10.1007/BF02534777 (1985).
31. Szklarczyk, D. *et al.* STRING v11: Protein–protein association networks with increased coverage, supporting functional discovery in genome-wide experimental datasets. *Nucleic Acids Res.* https://doi.org/10.1093/nar/gky1131 (2019).
32. Misra, H. P. & Fridovich, I. The univalent reduction of oxygen by reduced flavins and quinones. *J. Biol. Chem.* **247**, 188–192 (1972).
33. Sun, M. & Zigman, S. An improved spectrophotometric assay for superoxide dismutase based on epinephrine autoxidation. *Anal. Biochem.* https://doi.org/10.1016/0003-2697(78)90010-6 (1978).
34. Halliwell, B. & Foyer, C. H. Properties and physiological function of a glutathione reductase purified from spinach leaves by affinity chromatography. *Planta* **139**, 9–17 (1978).
35. Bowen, J. E. Physiology of genotypic differences in zinc and copper uptake in rice and tomato. *Plant Soil* https://doi.org/10.1007/BF02370159 (1987).
36. Hajiboland, R. & Amirazad, F. Growth, photosynthesis and antioxidant defense system in Zn-deficient red cabbage plants. *Plant, Soil Environ.* https://doi.org/10.17221/207/2009-pse (2010).
37. Su, L. *et al.* Interaction of zinc and IAA alleviate aluminum-induced damage on photosystems via promoting proton motive force and reducing proton gradient in alfalfa. *BMC Plant Biol.* https://doi.org/10.1186/s12870-020-02643-6 (2020).
38. Begum, M. C. *et al.* Biochemical and molecular responses underlying differential arsenic tolerance in rice (*Oryza sativa* L.). *Plant Physiol. Biochem.* https://doi.org/10.1016/j.plaphy.2016.03.034 (2016).
39. Impa, S. M. *et al.* Internal Zn allocation influences Zn deficiency tolerance and grain Zn loading in rice (*Oryza sativa* L.). *Front. Plant Sci.* **4**, 2 (2013).
40. Assuncao, A. G. L. *et al.* Arabidopsis thaliana transcription factors bZIP19 and bZIP23 regulate the adaptation to zinc deficiency. *Proc. Natl. Acad. Sci.* **107**, 10296–10301 (2010).
41. Choi, S., Hu, Y.-M., Corkins, M. E., Palmer, A. E. & Bird, A. J. Zinc transporters belonging to the cation diffusion facilitator (CDF) family have complementary roles in transporting zinc out of the cytosol. *PLOS Genet.* **14**, e1007262 (2018).
42. Mousavi, S. R. Zinc in crop production and interaction with phosphorus. *Aust. J. Basic Appl. Sci.* **5**, 1503–1509 (2011).
43. Rengel, Z. & Römheld, V. Root exudation and Fe uptake and transport in wheat genotypes differing in tolerance to Zn deficiency. *Plant Soil* **222**, 25–34 (2000).
44. Dubeaux, G., Neveu, J., Zelazny, E. & Vert, G. Metal sensing by the IRT1 transporter-receptor orchestrates its own degradation and plant metal nutrition. *Mol. Cell* **69**, 953-964.e5 (2018).
45. Van De Mortel, J. E. *et al.* Large expression differences in genes for iron and zinc homeostasis, stress response, and lignin biosynthesis distinguish roots of *Arabidopsis thaliana* and the related metal hyperaccumulator *Thlaspi caerulescens*. *Plant Physiol.* https://doi.org/10.1104/pp.106.082073 (2006).
46. Abreu, I. *et al.* Medicago truncatula Zinc-Iron Permease6 provides zinc to rhizobia-infected nodule cells. *Plant. Cell Environ.* **40**, 2706–2719 (2017).
47. Liu, X. S. *et al.* OsZIP1 functions as a metal efflux transporter limiting excess zinc, copper and cadmium accumulation in rice. *BMC Plant Biol.* https://doi.org/10.1186/s12870-019-1899-3 (2019).
48. Wang, Y., Blatt, M. R. & Chen, Z.-H. Ion Transport at the Plant Plasma Membrane. in *eLS* 1–16 (American Cancer Society, 2018). doi:https://doi.org/https://doi.org/10.1002/9780470015902.a0001307.pub3.
49. Du, J. *et al.* SlbHLH068 interacts with FER to regulate the iron-deficiency response in tomato. *Ann. Bot.* **116**, 23–34 (2015).
50. Kobayashi, T., Nozoye, T. & Nishizawa, N. K. Iron transport and its regulation in plants. *Free Radic. Biol. Med.* https://doi.org/10.1016/j.freeradbiomed.2018.10.439 (2019).
51. Ling, H.-Q., Bauer, P., Bereczky, Z., Keller, B. & Ganal, M. The tomato fer gene encoding a bHLH protein controls iron-uptake responses in roots. *Proc. Natl. Acad. Sci.* **99**, 13938–13943 (2002).
52. Yuan, Y. *et al.* FIT interacts with AtbHLH38 and AtbHLH39 in regulating iron uptake gene expression for iron homeostasis in *Arabidopsis*. *Cell Res.* **18**, 385–397 (2008).
53. Wang, N. *et al.* Requirement and functional redundancy of Ib subgroup bHLH proteins for iron deficiency responses and uptake in *Arabidopsis thaliana*. *Mol. Plant* **6**, 503–513 (2013).
54. Niu, L. & Liao, W. Hydrogen peroxide signaling in plant development and abiotic responses: Crosstalk with nitric oxide and calcium. *Front. Plant Sci.* **7**, 230 (2016).
55. Gupta, S. D., Agarwal, A. & Pradhan, S. Phytostimulatory effect of silver nanoparticles (AgNPs) on rice seedling growth: An insight from antioxidative enzyme activities and gene expression patterns. *Ecotoxicol. Environ. Saf.* **161**, 624–633 (2018).
56. Hacisalihoglu, G., Hart, J. J., Wang, Y.-H., Cakmak, I. & Kochian, L. V. Zinc efficiency is correlated with enhanced expression and activity of zinc-requiring enzymes in wheat. *Plant Physiol.* **131**, 595–602 (2003).
57. Kohli, S. K. *et al.* Assessment of subcellular ROS and NO metabolism in higher plants: Multifunctional signaling molecules. *Antioxidants* https://doi.org/10.3390/antiox8120641 (2019).

Acknowledgements
We would like to show our gratitude to Invent Technologies, Bangladesh.

Author contributions
Conceptualization, A.H.K. and M.S.A.; methodology, A.H.K.; software, U.D. and M.B.; validation, M.S.A., G.S. and M.S.; formal analysis, A.H.K.; investigation, A.H.K., M.S.A. and U.D.; resources, A.H.K.; data curation, A.H.K., M.S. and G.G.; writing—original draft preparation, A.H.K.; writing—review and editing, A.H.K., M.S., G.G., M.M.H.; visualization, A.H.K. and G.G.; supervision, A.H.K. and M.M.H.; project administration, A.H.K. and M.S., funding acquisition, A.H.K., M.S. and M.B. All of the authors contributed to the writing of the final version and approved the manuscript.

Funding
This work was supported by the Ministry of Education, Youth and Sports of the Czech Republic grant number (S grant of MSMT CR).

Competing interests
The authors declare no competing interests.

Additional information
Supplementary Information The online version contains supplementary material available at https://doi.org/10.1038/s41598-021-85649-w.

Correspondence and requests for materials should be addressed to A.H.K. or M.S.

Reprints and permissions information is available at www.nature.com/reprints.

Publisher's note Springer Nature remains neutral with regard to jurisdictional claims in published maps and institutional affiliations.